Available online at www.sciencedirect.com
ScienceDirect
Journal of Power Sources 161 (2006) 885–892
JOURNAL OF POWER SOURCES
www.elsevier.com/locate/jpowsour

A semi empirical model of the direct methanol fuel cell. Part II. Parametric analysis

K. Scott*, C. Jackson, P. Argyropoulos

Chemical Engineering and Advanced Materials, University of Newcastle upon Tyne, Merz Court, Newcastle upon Tyne, NE1 7RU, UK

Received 31 October 2005; received in revised form 29 March 2006; accepted 30 April 2006
Available online 22 June 2006

Abstract

A parametric analysis of a model equation developed to predict the cell voltage versus current density response of a liquid feed direct methanol fuel cell is presented. The equation is based on a semi-empirical approach in which methanol oxidation and oxygen reduction kinetics are combined with effective mass transport coefficients for the fuel cell electrodes. The model equation is applied to experimental data for a small-scale fuel cell and produces electrochemical parameters generally consistent with those expected for the individual components of the fuel cell MEA. The parameters thus determined are also used in the model to predict the performance of a DMFC with a new membrane electrode assembly.

Keywords: Direct methanol fuel cell; Cell performance; Empirical equation

1. Introduction

Previous models of the DMFC have been few. A one-dimensional model of the potential distribution and concentration distribution of methanol in the anode electrocatalyst layer was used in a model of the overall cell voltage performance of a vapour feed system [1,2]. The model gives good agreement with experimental data except under conditions where mass transport becomes rate limiting. Baxter et al. [3] have presented a model of the DMFC anode which is considered to be a porous electrode consisting of an electronically conducting catalyst structure that is thinly coated with an ion-selective polymer electrolyte. The pores of the electrode are filled with aqueous methanol solution in which all species of the reaction are free to transport. Mass transfer in the anode is defined in terms of a pseudo-mass transport coefficient. Other models have ignored current and potential distributions occurring in the electrocatalyst structures and considered the mass transport processes of methanol in the cell and the effect on electrode performance [4]. Recently we have considered the applicability of empirical models, originally developed for hydrogen polymer electrolyte fuel cells (PEMFC) [5].

The main drawback of the empirical equations derived for the PEMFC [6–9] was their inability to explain theoretically the values of parameters used to fit the data. In the first part of this paper [10] we confirmed the general ability of the semi-empirical model to predict experimental data. In this paper we consider the components of the model in detail and perform a parametric analysis of the coefficients obtained. The model is then used to predict the behaviour of a new DMFC.

2. Experimental

Tests on the DMFC were performed with a cell with a cross-sectional area of 9 cm^2. The cell consisted of two non-porous graphite blocks with a series of parallel channels machined into the block for the flow of methanol and oxygen/air (Fig. 1).

The cell was fitted with a membrane electrode assembly (MEA) sandwiched between the two graphite blocks. The cell was held together between two plastic insulation sheets and two stainless steel backing plates using a set of retaining bolts positioned around the periphery of the cell. Electrical heaters, supplied by Watson Marlow, were placed behind each of the graphite blocks to heat the cell to the desired operating temperature. The graphite blocks were also provided with electrical contacts and small holes to accommodate thermocouples. The fuel cells were used in a simple flow rig, which consisted of

* Corresponding author. Tel.: +44 1912228771; fax: +44 1912225292.
E-mail address: k.scott@ncl.ac.uk (K. Scott).

0378-7753/$ – see front matter © 2006 Elsevier B.V. All rights reserved.
doi:10.1016/j.jpowsour.2006.04.147

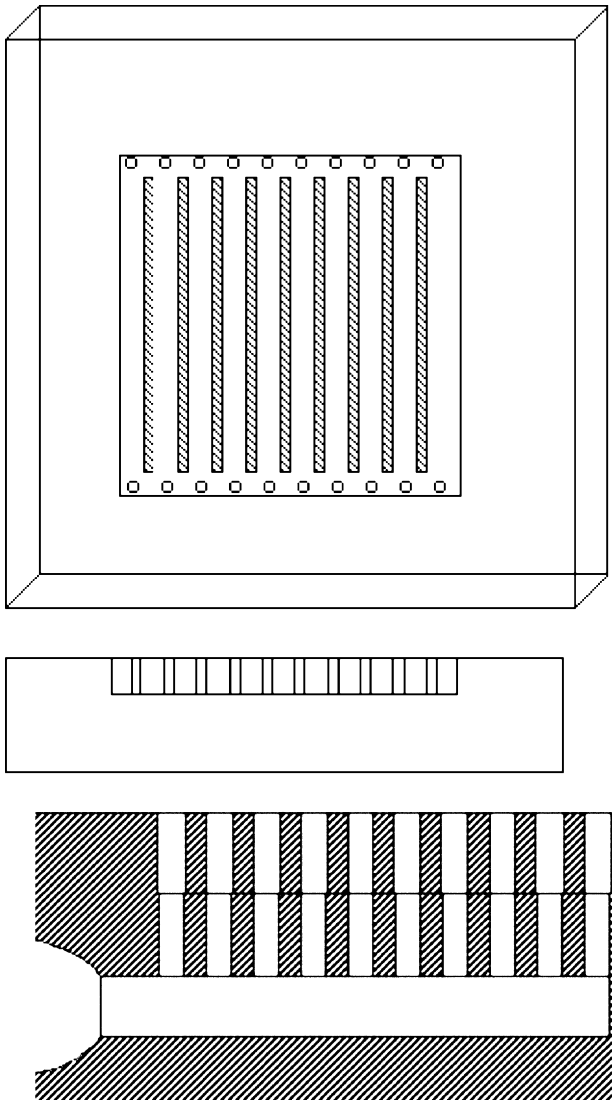

Fig. 1. DMFC small-scale cell flow bed design and manifold arrangement.

a Watson Marlow peristaltic pump to supply aqueous methanol solution, from a reservoir, to a Eurotherm temperature controller to maintain the cell at a constant temperature. Air was supplied from cylinders, at ambient temperature, and the pressure regulated by needle valves.

MEAs studied in this work were made in the following manner: the anode consisted of a Teflonised (20%) carbon cloth support (E-Tek, type 'A'), of 0.3 mm thickness, upon which was spread a thin (diffusion layer) layer of uncatalysed (ketjenblack 600) 10 wt.% Teflonised carbon. The catalysed layer, unless otherwise specified consisted of 35 wt.% Pt–15 wt.% Ru (2 mg cm^{-2} metal loading) dispersed on carbon (ketjen) and bound with bound with 10 wt.% Nafion® from a solution of 5 wt.% Nafion® dissolved in a mixture of water and lower aliphatic alcohol's (Aldrich), was spread on this diffusion backing layer. A thin layer of Nafion® solution was spread onto the surface of each electrode. The cathode was constructed using a similar method as for the anode, using a thin diffusion layer bound with 10 wt.% PTFE, and 1 mg cm^{-2} Pt black with 10 wt.% Nafion® in the catalyst layer. The electrodes were placed either side of a pre-treated Nafion® 117 membrane. This pre-treatment involved boiling the membrane for 1 h in 5 vol.% H_2O_2 and 1 h in 1 mol dm^{-3} H_2SO_4 before washing in boiling Millipore water (>18 mΩ) for 2 h with regular changes of water. The assembly was hot-pressed at 100 kg cm^{-2} for 3 min at 135 °C.

Cell voltage versus current density response was measured galvanostatically, by incrementally increasing the current from open circuit and measuring the cell potential and then reducing the current incrementally again measuring the cell voltage. The data reported here were obtained with one MEA, unless otherwise stated. The MEA was conditioned before use in two stages: for 48 h in the test cell, in 2.0 mol dm^{-3} methanol solution at 75 °C, and then by maintaining the cell with an applied load of 100 mA cm^{-2} for several hours. This pre-treatment resulted in stable performance under continuous operation.

3. Model equation

As a kinetic model for methanol oxidation, Tafel type kinetics is chosen:

$$j = j_0 \frac{(C^{\mathrm{a}}_{\mathrm{ME}})^N}{C^{\mathrm{ref}}_{\mathrm{ME}}} \exp\left[\frac{\alpha_{\mathrm{a}} F}{RT}(E - E_0)\right] \tag{1}$$

where j_0 is the exchange current at the reference concentration, α the transfer coefficient, "a" refers to the condition at the anode catalyst surface and N is an order of reaction.

We represent mass transport in the anode side of the cell using the effective mass transport coefficient, k_{eff}:

$$j = k_{\mathrm{eff}} n F (C_{\mathrm{ME}} - C^{\mathrm{a}}_{\mathrm{ME}}) \tag{2}$$

By re-arranging the previous Eq. (1) the overpotential becomes:

$$(E - E_0)_{\mathrm{anode}} = \frac{RT}{\alpha_{\mathrm{a}} F}\left[\ln\frac{j}{(C^{\mathrm{a}}_{\mathrm{ME}})^N} - \ln\frac{j_0}{C^{\mathrm{ref}}_{\mathrm{ME}}}\right] \tag{3}$$

By combining Eqs. (2) and (3) we obtain:

$$(E - E_0)_{\mathrm{anode}} = \frac{RT}{\alpha_{\mathrm{a}} F}\left[\ln\frac{jC^{\mathrm{ref}}_{\mathrm{ME}}}{j_0 (C_{\mathrm{ME}})^N} - N\ln\left(1 - \frac{j}{nFk_{\mathrm{eff}} C_{\mathrm{ME}}}\right)\right] \tag{4}$$

Using Eq. (4) for the anode we can obtain an expression for the cell voltage by introducing the kinetic expression for oxygen reduction:

$$j = j_{0\mathrm{c}}\left[\frac{{p_{\mathrm{O}}}^{N_{\mathrm{O}}}}{p^{\mathrm{ref}}_{\mathrm{O}}} \exp\left(-\frac{\alpha_{\mathrm{c}} F \eta_{\mathrm{c}}}{RT}\right)\right] \tag{5}$$

where p_{O} is the partial pressure for oxygen and N_{O} is the reaction order for oxygen reduction.

The cathode overpotential is then

$$(E - E_0)_{\mathrm{cathode}} = \frac{RT}{\alpha_{\mathrm{c}} F}\left[\ln\frac{jp^{\mathrm{ref}}_{\mathrm{O}}}{j_{0\mathrm{c}} (p_{\mathrm{O}})^{N_{\mathrm{O}}}} - N_{\mathrm{O}}\ln\left(1 - \frac{j}{nFk_{\mathrm{lO}} p_{\mathrm{O}}}\right)\right] \tag{6}$$

where k_{lO} is the mass transport coefficient for the cathode side of the cell.

Combining Eqs. (4) and (6), we obtain an expression for the cell voltage, E_{cell}, as

$$E_{cell} = E_{Ocell} - R_e j - \frac{RT}{F}\left(\frac{1}{\alpha_a} + \frac{1}{\alpha_c}\right)\ln j - \frac{RT}{\alpha_c F} \times \left[\ln\frac{p_O^{ref}}{j_{0c}(p_O)^{N_O}} - N_O \ln\left(1 - \frac{j}{nFk_{lO}p_O}\right)\right] - \frac{RT}{\alpha_a F} \times \left[\ln\frac{C_{ME}^{ref}}{j_0(C_{ME})^N} - N\ln\left(1 - \frac{j}{nFk_{eff}C_{ME}}\right)\right] \quad (7)$$

To model the performance of the DMFC we propose the following semi-empirical equation for the cell voltage, E_{cell}, in which we assume that the reduction of oxygen does not proceed under mass transport limitations:

$$E_{cell} = E_O^* - b_{cell}\log j - R_e j + C_1 \ln(1 - C_2 j) \quad (8)$$

where

$$b_{cell} = \frac{2.303RT}{F}\left(\frac{1}{\alpha_a} + \frac{1}{\alpha_c}\right), C_1 = \frac{NRT}{\alpha_a F}, C_2 = \frac{1}{nFk_{eff}C_{ME}},$$

$$E_O^* = E_{Ocell} - \frac{RT}{\alpha_c F}\ln\left(\frac{p_O^{ref}}{j_{Oc}(p_O)^{N_O}}\right) - \frac{RT}{\alpha_a F}\ln\left(\frac{C_{ME}^{ref}}{j_0 C_{ME}^N}\right)$$

In the above j is the current density, α_a and α_c the transfer coefficients for the oxidation of methanol and reduction of oxygen, respectively, R_e the internal cell resistance (mainly due to the polymer electrolyte membrane), N a reaction order for methanol oxidation, k_{eff} an effective mass transport coefficient for the anode side of the cell, C_{ME} the methanol concentration and p_O is the oxygen pressure. E_{Ocell} is the standard potential for the DMFC overall reaction, which theoretically is given by the Nernst equation.

4. Application of the model

In the previous paper [10] we confirmed the general applicability of the model Eq. (1) to represent the cell voltage, current density behaviour of the DMFC.

The proposed model was used to predict the voltage response of a specific small-scale DMFC cell when operated under constant cathodic overpressure with air fed at a constant rate, and with the anode side solution flow rate also constant at 1.12 $cm^3\ min^{-1}$. In doing so we tried to minimise the effects that are attributable to changes in the cathode side overpressure or due to an increased methanol solution flow rate. Both parameters under specific circumstances can alter the cell response [11–17].

Fig. 2 indicates that the open cell voltage decreases, by approximately 0.05 V, with increasing methanol solution concentration from 0.25 to 0.5 M, as the impact of methanol crossover on cathode performance becomes more significant. The variation in E_O^* is consistent with that as proposed in the model Eq. (1). Open circuit potential also increases with increasing temperature as expected due to more catalyst activity and as predicted from the Nernst equation. These are general trends and a more detailed theoretical approach can be found below in the relative section.

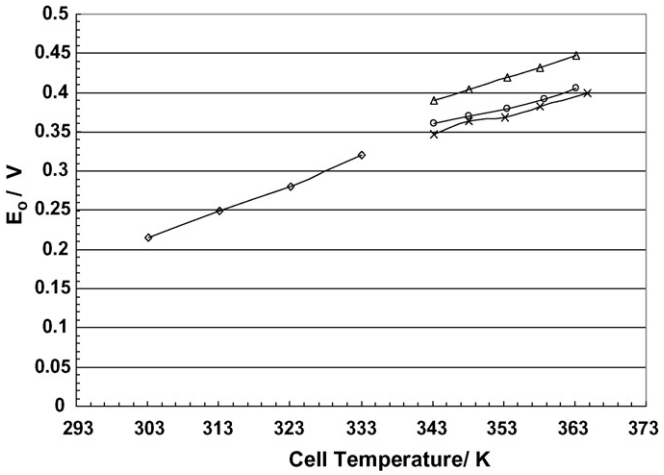

Fig. 2. Fitted values for parameter E_O^* of Eq. (8) as a function of cell temperature in K for a cell operated with various methanol solutions (methanol solution concentrations, △: 0.125 M; ◯: 0.25 M; ×: 0.5 M; ◊: 0.75 M) supplied at a rate of 1.12 $cm^3\ min^{-1}$ with air fed cathodes pressurised at 2 bar.

Fig. 3 shows the combined effect of methanol solution concentration and temperature on the effective Tafel slope b_{cell}. As it can be seen Tafel slope increases with an increase in cell temperature and is not influenced by methanol solution concentration to a significant extent. The effect of temperature is consistent with that predicted by the model. For example an increase in temperature from 303 to 363 K gives an approximate 20% increase in the value of b_{cell} (0.108–0.124). It should be noted here that an increase in methanol solution concentration is not expected to effect of value of b_{cell} unless of course then is an influence brought about by methanol crossover.

Fig. 4 shows the combined effect of methanol solution concentration and temperature on cell resistance R. The effect of

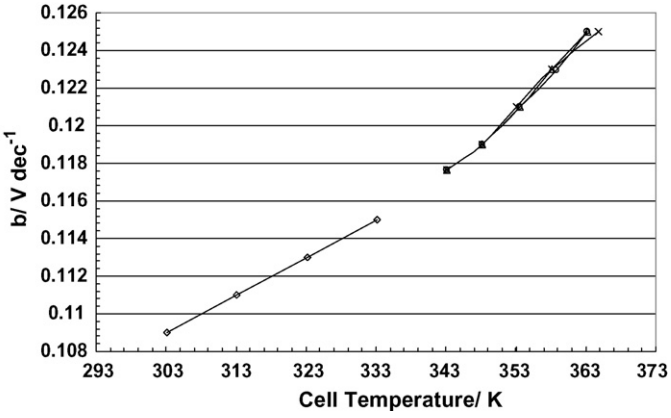

Fig. 3. Fitted values for parameter b_{cell} of Eq. (1) as a function of cell temperature in K for a cell operated with various methanol solution concentrations, supplied at a rate of 1.12 $cm^3\ min^{-1}$ with air fed cathodes pressurised at 2 bar (△: 0.125 M; ◯: 0.25 M; ×: 0.5 M; ◊: 0.75 M).

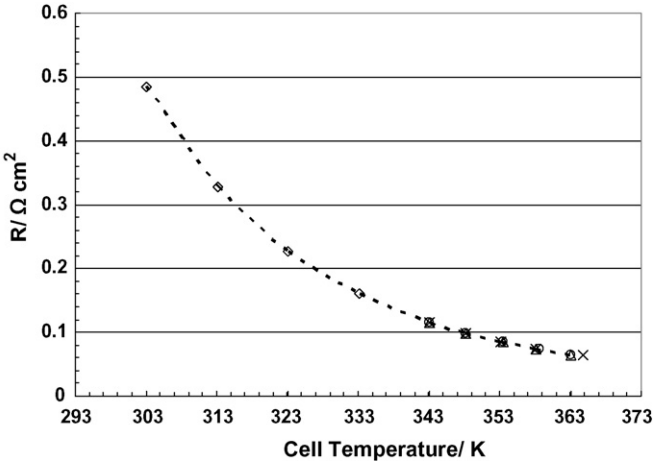

Fig. 4. Fitted values for parameter R of Eq. (1) as a function of cell temperature in K for a cell operated with various methanol solutions (methanol solution concentrations, △: 0.125 M; ◯: 0.25 M; ×: 0.5 M; ◇: 0.75 M) supplied at a rate of 1.12 $cm^3\ min^{-1}$ with air fed cathodes pressurised at 2 bar.

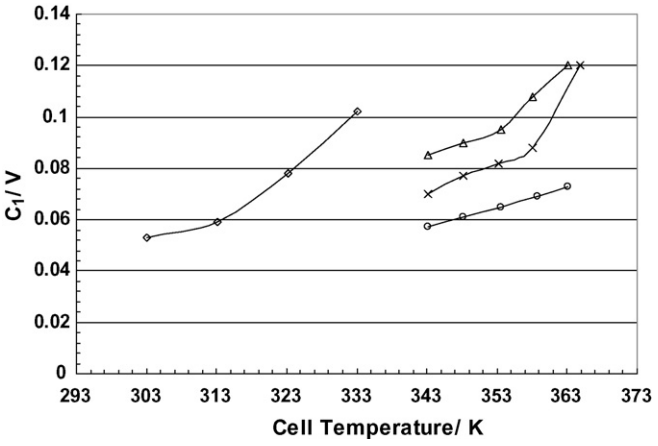

Fig. 5. Fitted values for parameter C_1 of Eq. (8) as a function of cell temperature in K for a cell operated with various methanol solutions (methanol solution concentrations, △: 0.125 M; ◯: 0.25 M; ×: 0.5 M; ◇: 0.75 M) supplied at a rate of 1.12 $cm^3\ min^{-1}$ with air fed cathodes pressurised at 2 bar.

methanol solution concentration on resistance R is negligible in the concentration range considered. The effect of temperature is to decrease the resistance as expected from known correlations for the resistivity of Nafion^{TM} membranes. The resistivity of Nafion over the temperature range considered in Fig. 4 is consistent with published data. For example at 80 °C the protonic conductivity is 0.202 S cm^{-1} which with a 170 μm thick membrane gives a resistivity of approximately 0.085 Ω cm^2, which compares favourably with the data in Fig. 4.

The values of resistivity are correlated by the expression:

$$R = R_0 \exp\left(\frac{B}{T} - \frac{B}{T_0}\right) \tag{9}$$

$R_0 = 0.085\ \Omega\ cm^2$ is the resistance at a temperature $T_0 = 383.15$ K and $B = 3724$ is a constant determined from the existing data set (see dotted line in Fig. 3). Hence in the model Eq. (9) the resistance parameter can be fixed, with a function following the trend indicated in Fig. 3, and thus reduces the number of fitting parameters in the model. It should be noted that part of the cell resistance is not due to the Nafion membrane.

Fig. 5 shows the combined effect of methanol solution concentration and temperature on the model parameter C_1. As predicted, the value of C_1 increases with increasing temperature. The effect of methanol concentration is to produce a minimum value of coefficient C_1 at a particular temperature. This behaviour is oxidation is not a simple electrochemical process and that the Tafel kinetic equation is indeed an approximation. It has been reported that the reaction order for methanol is difficult to explain in terms of the model equation. A contributing factor will be that the reaction order for methanol oxidation is 1.0 at low concentrations and decreases to zero at higher concentrations of around 2.0 M. The variation in reaction order itself depends upon the electrode potential. In terms of actual coefficient values, it is expected that these would be closely linked to the Tafel slope for the reaction ($RT/\alpha_a F$). For example at a temperature of 343 K and with a transfer coefficient, of 0.5 and a reaction order, $N = 1.0$, the coefficient C_1 has a value of approximately 0.06 V. This value agrees with the computed ("best fit") value obtained from the data analysis as shown in Section 6 later.

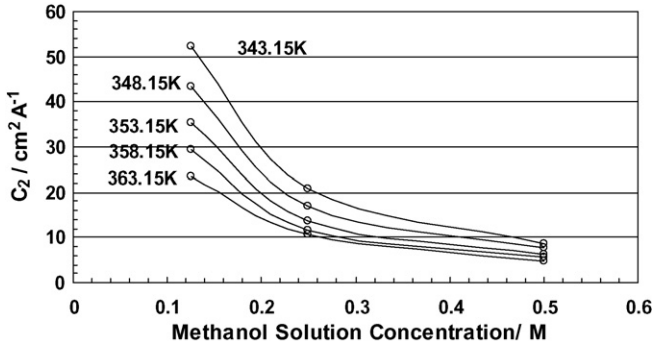

Fig. 6. Fitted values for parameter C_2 of Eq. (1) as a function of aqueous methanol solution concentrations in M for five different cell temperatures.

Fig. 6 shows the combined effect of methanol solution concentration and temperature on model parameter C_2. From the definition of this parameter it is expected that an increase in methanol concentration would decrease the value of C_2, which is confirmed in Fig. 5. In addition the observed decrease in the value of C_2 with temperature is expected due to an increase in the value of mass transport coefficient at higher temperature: a diffusion-related effect. We explore the relationship between the model coefficients and kinetic and mass transport parameters in more detail below.

5. Effective mass transfer coefficients

The variation in effective mass transfer coefficient with temperature is partly due to an increase in methanol diffusion coefficient with temperature. An additional effect created by the higher temperatures may be enhanced mass transport due to bubble liberation at the surface of the MEA. At higher temperatures a higher bubble velocity in the diffusion layers can

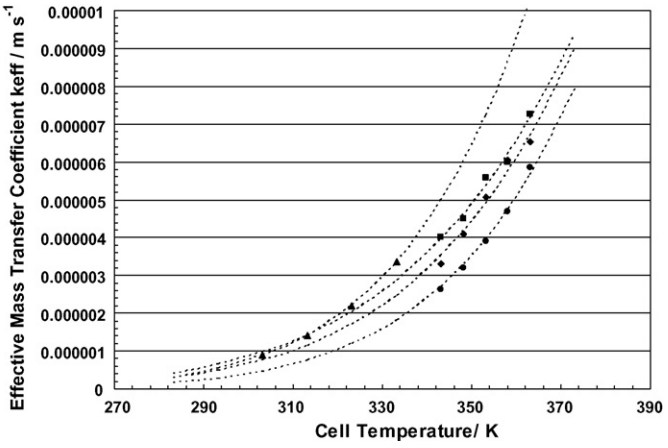

Fig. 7. Empirical equation and proposed model predicted effective mass transfer coefficients as a function of cell temperature in for a cell operated with various methanol solutions (methanol solution concentrations, ●: 0.125 M; ♦: 0.25 M; ■: 0.5 M; ▲:0.75 M) supplied at a rate of 1.12 cm^3 min^{-1} with air fed cathodes pressurised at 2 bar. Model predictions are presented with dotted lines.

lead to an increase in liquid voidage, which in turn increases the effective mass transfer in the carbon cloth. It is not known whether a higher rate of CO_2 generation (higher current density) increases the gas velocity in the cloth or increases the gas voidage in the cloth. In addition higher temperatures will increase the methanol and water transfer through the Nafion membrane, which will influence the mass transport rate of methanol at the anode.

The methanol concentration influences mass transport in several ways; at low methanol concentrations, limiting currents are lower and therefore lower gas evolution rates result. Lower gas evolution rates will reduce any hydrodynamic influence on the mass transport rate at the carbon cloth, or locally at the surface of the anode catalyst. The gas evolution rate will influence the voidage of the liquid in the carbon cloth, which will in turn affect the methanol diffusion rate. Lower methanol concentrations also reduce methanol transfer by diffusion and electro-osmosis, through the membrane, due to a lower current density of operation, which will also reduce the methanol transfer rate to the anode. The local temperature and pressure at the anode will also influence mass transport rates. Higher temperatures increase the local vaporisation rate of methanol into carbon dioxide gas formed at the anode, which will reduce the effective liquid phase concentration.

Fig. 7 shows the variation of effective mass transfer coefficient with cell temperature and methanol solution concentration. Mass transfer coefficients increase with an increase in temperature and with methanol concentration. The latter effect is essentially due to the higher limiting current densities at the higher concentrations, which cause a greater evolution of carbon dioxide gas. The data in Fig. 7 can be correlated by the expression:

$$k_{\text{eff}} = k_{\text{lo}} C_{\text{ME}}{}^{a} \exp\left(-\frac{A}{T}\right) \quad (10)$$

where k_{lo}, a and A are constants with the following values:

	0.125	0.25	0.5	0.75
k_{lo}	14.47349235	1.695694434	0.3563206632	3.342514414
A	4601.967164	4014.656868	3675.977493	4505.215133

The prediction of Eq. (10) are compared with the experimental variation of mass transfer coefficient with methanol concentration as a function of cell temperature, in Fig. 7.

6. Empirical equation-based kinetic parameter

Fig. 8 shows the variation in the combined transfer coefficients alpha, $\alpha_a\alpha_c/(\alpha_a+\alpha_c)$, as obtained from the value of the coefficient b_{cell}. As can be seen the variation in the coefficient with methanol concentration is small. The value indicates that the transfer coefficients for one or both cell reactions are greater than 0.5 and potentially close to 1.0. The effect of temperature is to increase the value of alpha by approximately 5% over the range 300–350 K and thus within experimental error an approximate constant value can be assumed as reasonable.

6.1. Application of the model

Recently we have reported an improved performance DMFC operating under ambient air conditions [19]. The improved performance was based on an improved MEA fabrication procedure using a carbon paper backing layer. We have applied the model discussed in this paper to the data as shown in Figs. 9 and 10. As can be seen there is good agreement between the model and experiment.

The Tafel slope and the cell resistance (parameters b and R in the proposed empirical equation) were kept constant and the same for the cell tested in the present paper. Although the performance of the cell with the modified MEA is significantly better, the cathode pressure is ambient and methanol concentration is higher (1.0 M) the model still describes the cell behaviour quite

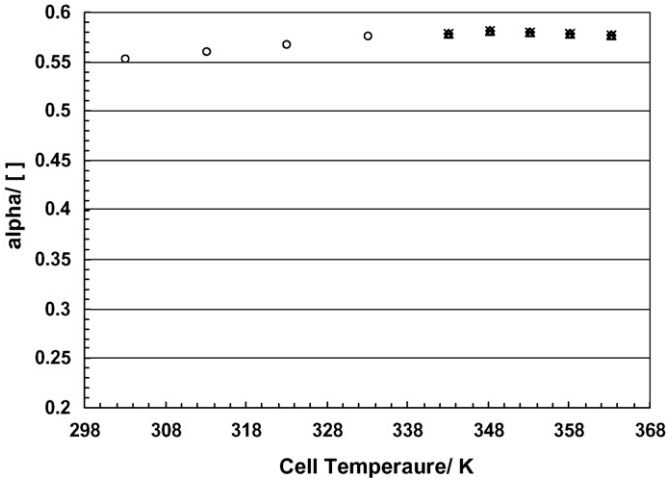

Fig. 8. Empirical equation-based predicted values for the kinetic related parameter α as a function of cell temperature for different methanol solution concentrations (◇: 0.125 M; ×: 0.25 M; △: 0.5 M; ◯: 0.75 M).

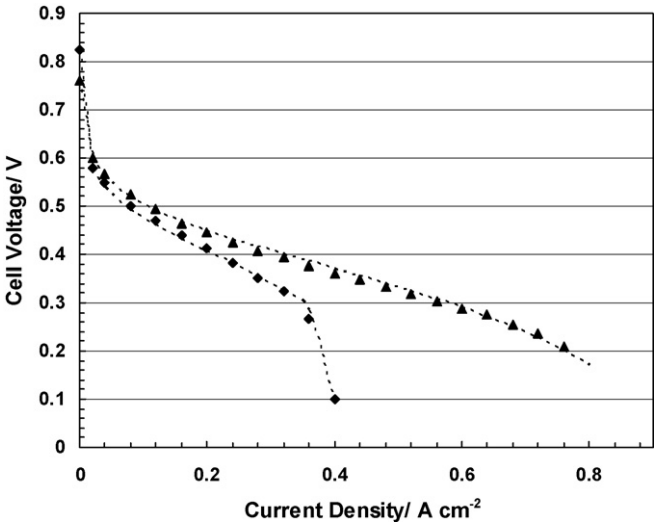

Fig. 9. Demonstration of the empirical equation to an oxygen fed DMFC with different MEA fabrication technique. The cell is operated at ambient pressure with 1.0 M aqueous methanol solution (cell temperature: ♦: 60 °C; ▲: 90 °C).

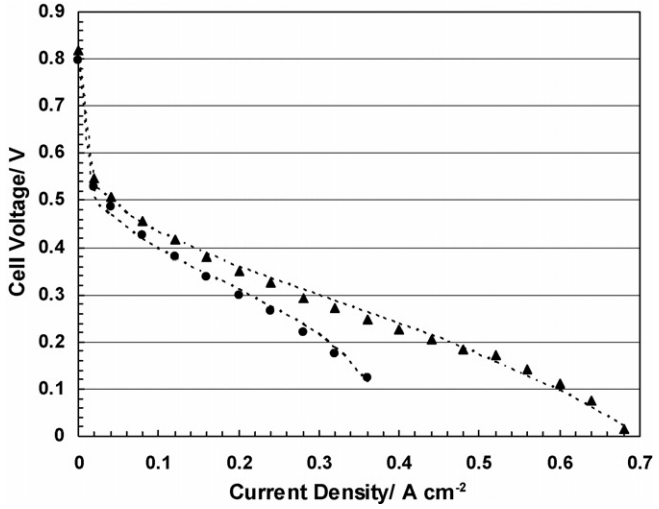

Fig. 10. Demonstration of the proposed empirical equation to an air fed DMFC with different MEA fabrication technique. The cell is operated at ambient pressure with 1.0 M aqueous methanol solution (cell temperature: ♦: 60 °C; ▲: 90 °C).

accurately. The values of the coefficients used to fit the data are given in Table 1.

Comparing the parameters C_1 and C_2 for both sets of experimental data we see that there are some significant differences. In the case of C_2 which is inversely proportional to the product of methanol concentration and effective mass transport coefficient, the values are higher for the new cell design. For example at 60 and 90 °C the values are 0.9 and 0.45, respectively (for 0.75 M methanol), with the original cell design compared to 2.5 and 1.05 for the new cell design. That is, effective mass transport coefficients for the new design are approximately twice those of the original cell design.

Table 1
Model parameters for the improved fuel cell performance

	O_2 (60 °C)	O_2 (90 °C)	Air (60 °C)	Air (90 °C)
E_0 (V)	0.39	0.395	0.33	0.34
b (V dec^{-1})	0.11	0.124	0.11	0.124
R (Ω cm^2)	0.192	0.0225	0.192	0.0225
C_1 (V)	0.058	0.12	0.085	0.126
C_2 (cm^2 A^{-1})	2.5	1.05	2.5	1.05

The values of C_1 at 90 °C are similar for both sets of data at the two temperatures. The variations in the values of C_1 at 60 °C are more difficult to explain, i.e. approximately 0.1 for the original cell design with air and now 0.085 for air and 0.058 for air and oxygen, respectively. However, the term C_1 is essentially a multiplier on the mass transport limiting component of the empirical equation and thus variations in the values are indicative of differences in cell design.

7. Open cell voltage modelling

In theory the open circuit potential (or rather the equilibrium potential) for the DMFC is given by the Nernst equation:

$$E_{OC} = E^0 + \frac{RT}{6F}\ln\left(\frac{a_{CH_3OH}(y_{O_2,air}p_{cath})^{3/2}}{p_{CO_2}}\right) \quad (11)$$

where E_{OC} is the cell voltage (V), E^0 the standard cell voltage (V), a_{CH_3OH} the activity of methanol in solution, $y_{O_2,air}$ the mole fraction of oxygen in air (−), p_{cath} the cathodic gas pressure (Pa), and p_{CO_2} is the partial pressure carbon dioxide (Pa).

However, it is known that as well as interfacial phenomena affecting the vale of E_0 a major factor is that of methanol crossover which depolarises the cathode. This causes a significant reduction in potential from that predicted by the Nernst equation. As a model of the cathode of the DMFC we base this on a mixed potential for oxygen reduction and methanol oxidation.

As a basis we adopt Butler Volmer kinetics for methanol oxidation and oxygen reduction in the following form, which were used as a basis for the empirical non-equilibrium model:

$$j_{ME} = j_0\frac{(C_{ME})^N}{C_{ME}^{ref}}\exp\left[\frac{\alpha_a F\eta_a}{RT}\right] - \frac{P_{CO_2}}{P_{CO_2ref}}\exp\left[\frac{-\alpha_a F\eta_a}{RT}\right] \quad (12)$$

$$j_{O_2} = j_{0c}\left[\frac{(p_O)^{N_O}}{p_O^{ref}}\left(\exp\left(-\frac{\alpha_c F\eta_c}{RT}\right) - \exp\left(\frac{\alpha_c F\eta_a}{RT}\right)\right)\right] \quad (13)$$

where $\eta_a = E_{0c} - E^0_{ME}$ and $\eta_c = E_{0c} - E^0_{O_2}$ and P_{CO_2} refers to pressure of carbon dioxide product and C_{ME} refers to the methanol concentration at the cathode which will be determined by the overall rate of transport of methanol through the MEA.

We now consider that the total current at the cathode is the sum of the methanol oxidation and oxygen reduction currents:

$$j = j_{ME} + j_{O_2} \quad (14)$$

Then apply equilibrium such that

$$j = 0 = j_{0c}\left[\frac{(p_O)^{N_O}}{p_O^{ref}}\left(\exp\left(-\frac{\alpha_c F\eta_c}{RT}\right) - \exp\left(\frac{\alpha_c F\eta_a}{RT}\right)\right)\right] + j_0\frac{(C_{ME})^N}{C_{ME}^{ref}}\exp\left[\frac{\alpha_a F\eta_a}{RT}\right] - \frac{P_{CO_2}}{P_{CO_2 ref}}\exp\left[\frac{-\alpha_a F\eta_a}{RT}\right] \quad (15)$$

With the assumption that the partial pressure of carbon dioxide will be small we simplify this to

$$j_{0c}\left[\frac{(p_O)^{N_O}}{p_O^{ref}}\left(\exp\left(-\frac{\alpha_c F\eta_c}{RT}\right) - \exp\left(\frac{\alpha_c F\eta_a}{RT}\right)\right)\right] = -j_0\frac{(C_{ME})^N}{C_{ME}^{ref}}\exp\left[\frac{\alpha_a F\eta_a}{RT}\right] \quad (16)$$

Re-arranging and taking logs gives

$$\ln(\exp(-\beta_{ME}\eta_a)(\exp(-\beta_c\eta_c) - \exp(\beta_c\eta_c))) = \ln\frac{j_0 p_O^{ref}}{j_{0c}(p_O)^{N_O}} + N_M\ln\left(\frac{C_{ME}}{C_{ME}^{ref}}\right) \quad (17)$$

where generally, $\beta = \alpha nF/RT$.

Hence

$$(-\beta_{ME}\eta_a) + \ln(\exp(-\beta_c\eta_c) - \exp(\beta_c\eta_c)) = \ln\frac{j_0 p_O^{ref}}{j_{0c}(p_O)^{N_O}} + N_M\ln\left(\frac{C_{ME}}{C_{ME}^{ref}}\right) \quad (18)$$

which gives

$$(-\beta_{ME}\eta_a) - \beta_c\eta_c + \ln(1 - \exp(2\beta_c\eta_c)) = \ln\frac{j_0 p_O^{ref}}{j_{0c}(p_O)^{N_O}} + N_M\ln\left(\frac{C_{ME}}{C_{ME}^{ref}}\right) \quad (19)$$

Under conditions when the cathode is significantly polarised by methanol (which occurs in practice) then from the definition of overpotential, noting that values of η_c are negative, we thus obtain:

$$(\beta_{ME} + \beta_c)E_{0c} = \beta_{ME}E_{ME}^0 + \beta_c E_{O_2}^0 - \ln\frac{j_0 p_O^{ref}}{j_{0c}(p_O)^{N_O}} - N_M\ln\left(\frac{C_{ME}}{C_{ME}^{ref}}\right) \quad (20)$$

In fact, several researchers have observed that the open circuit voltage decreases with increasing methanol concentration and that the cathode electrode performance was significantly lower at higher methanol concentration [4,18].

The model Eq. (5) states that the open circuit potential varies linearly with the log of methanol solution concentration according to

$$E_{0c} = \omega + \lambda\log C_{MeOH} \quad (21)$$

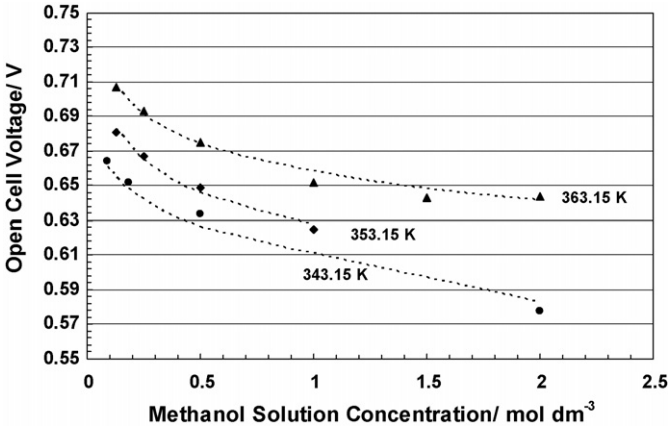

Fig. 11. Experimentally measured and model predicted (dotted lines) open cell voltage as a function of cell temperature (shown in figure) for a cell operated with various methanol concentrations supplied at a rate of 1.12 $cm^3\ min^{-1}$ with air fed cathodes pressurised at 2 bar.

where

$$\omega = \frac{\beta_{ME}}{\beta_c + \beta_{ME}}E_{ME}^0 + \frac{\beta_c}{\beta_c + \beta_{ME}}E_{O_2}^0 - \frac{1}{\beta_c + \beta_{ME}}\ln\left(\frac{j_0 p_O^{ref}}{j_{0c_o}(p_O)^{N_O}C_{ME}^{ref}}\right)$$

and

$$\lambda = -\frac{N_M}{\beta_{ME} + \beta_c}$$

which vary with temperature.

Fig. 11 shows a typical fit of Eq. (21) to experimental data at a fixed temperature. Agreement between model and data is quite reasonable with the coefficients shown on Fig. 12. The coefficient λ varies linearly with temperature and at 343 K the value is −0.02755. Hence from this the combined value of Tafel slopes as defined by b_{cell} is 0.63 which is comparable to, but smaller than, the value shown in Fig. 3 (assuming $N_{ME} = 1.0$). There are a number of factors, which would contribute to this disagreement in derived parameters but major factors will be the amount of experimental data and assumptions in the model.

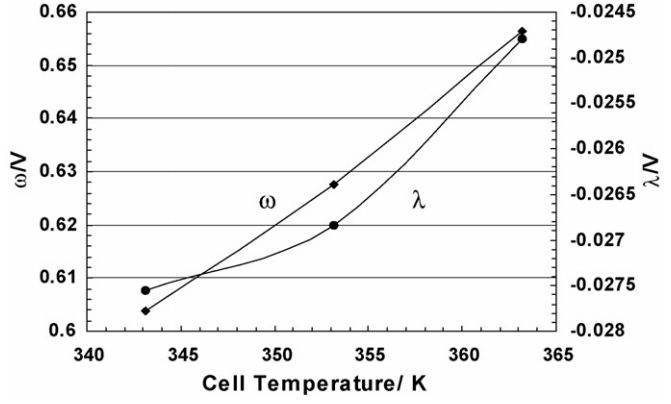

Fig. 12. Variation of the fitting coefficients for Eq. (6) as a function of cell temperature for the data used in Fig. 11.

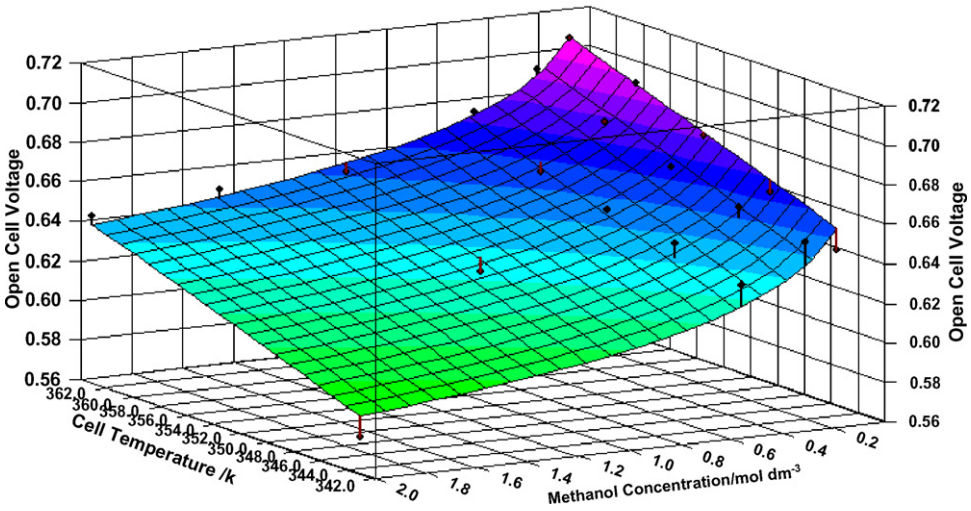

Fig. 13. Comparison of the model based predicted open cell voltage with actual experimental values obtained as a function of cell temperature and for various methanol solution concentrations supplied at a rate of 1.12 cm^3 min^{-1} with air fed cathodes pressurised at 2 bar.

The coefficient ω also varies linearly with temperature (over the range considered) as predicted by the model. Overall the variation in open circuit potential as predicted by the model is shown in Fig. 13.

8. Conclusions

Experimental data from a small-scale DMFC, operated over a range of temperatures and moderately low methanol solution concentrations, has been used to validate a semi-empirical model of the cell. The model parameters or coefficients have been determined by the best statistical fit to experimental data and have been used to determine approximate kinetic and mass transport related constants. The open circuit potential of the cell has been interpreted by a model based on a mixed potential associated with oxygen reduction and methanol oxidation at the cathode. The semi-empirical model of the DMFC has been used to model data from a new cell, which gives significantly higher power densities than the test cell used to validate the model.

Acknowledgements

The authors would like to acknowledge the following for support of this research: the European Commission for a TMR Marie Curie B20 and an IHP Marie Curie B30 research training grant to Dr. P. Argyropoulos; EPSRC supported Mr. C. Jackson through a PhD studentship.

References

[1] K. Scott, W.M. Taama, J. Cruickshank, Performance of a direct methanol fuel cell, J. Appl. Electrochem. 28 (3) (1998) 289–297.
[2] K. Scott, W.M. Taama, J. Cruickshank, Performance and modelling of a direct methanol solid polymer electrolyte fuel cell, J. Power Sources 65 (1–2) (1997) 159–171.
[3] S.F. Baxter, V.S. Battaglia, R.E. White, Methanol fuel cell: anode, J. Electrochem. Soc. 146 (2) (1999) 437–447.
[4] K. Sundmacher, K. Scott, Direct methanol polymer electrolyte fuel cell: analysis of charge and mass transfer in the vapour–liquid–solid system, Chem. Eng. Sci. 54 (13–14) (1999) 2927–2936.
[5] P. Argyropoulos, K. Scott, A.K. Shukla, C. Jackson, Investigation of the applicability of PEMFC derived empirical equations to DMFCs. A new empirical equation approach for DMFCs, Fuel Cells-Fund. Syst. 2 (2002) 78.
[6] J.H. Lee, T.R. Lalk, A.J. Appleby, Modelling electrochemical performance in large scale proton exchange membrane fuel cell stacks, J. Power Sources 70 (1998) 258–268.
[7] J.H. Lee, T.R. Lalk, A modelling technique for fuel cell stack systems, in: Proceedings of the ASME Dynamics Systems and Control Division, 1996.
[8] G. Squadrito, G. Maggio, E. Passalacqua, F. Lufrano, A. Patti, An empirical equation for polymer electrolyte fuel cell (PEFC) behaviour, J. Appl. Electrochem. 29 (1999) 1449–1455.
[9] J. Kim, S. Lee, S. Srinivansan, C.E. Chamberlin, Modeling of proton exchange membrane fuel cell performance with an empirical equation, J. Electrochem. Soc. 142 (8) (1995) 2670–2674.
[10] P. Argyropoulos, K. Scott, A.K. Shukla, C. Jackson, A semi empirical model for the direct methanol fuel cell. Part 1. Model development and verification, J. Power Sources 123 (2003) 190.
[11] P. Argyropoulos, K. Scott, W.M. Taama, Carbon dioxide evolution patterns in operating DMFC cells, Electrochim. Acta 44 (1999) 3575–3584.
[12] P. Argyropoulos, K. Scott, W.M. Taama, Gas evolution and power performance in direct methanol fuel cells, J. Appl. Electrochem. 29 (1999) 661–669.
[13] W.M. Taama, P. Argyropoulos, K. Scott, Parametric studies on the liquid feed DMFC, in: Proceedings of the 1998 IChemE Research Event, IChemE, Newcastle upon Tyne, 1998.
[14] K. Scott, W.M. Taama, P. Argyropoulos, Mass transport and flow visualisation in the direct methanol fuel cell, in: Proceedings of the Electrochem 99, Portsmouth, UK, 1999.
[15] K. Scott, W.M. Taama, P. Argyropoulos, Engineering aspects of the direct methanol fuel cell system, J. Power Sources 79 (1) (1999) 43–59.
[16] K. Scott, W.M. Taama, P. Argyropoulos, Material aspects of the liquid feed direct methanol fuel cell, J. Appl. Electrochem. 28 (12) (1999) 1389–1397.
[17] K. Scott, P. Argyropoulos, Flow and mass transport in direct methanol fuel cells, Int. J. Transport Phenom. 3 (2001) 257.
[18] M.K. Ravikumar, A.K. Shukla, Effect of methanol crossover in a liquid feed polymer electrolyte direct methanol fuel cell, J. Electrochem. Soc. 143 (8) (1996) 2601–2606.
[19] A. Shukla, K. Scott, C. Jackson, An improved performance liquid feed solid polymer electrolyte direct methanol fuel cell, Electrochim. Acta 111 (2002) 43.